

Investigation of complete and incomplete fusion in $^{20}\text{Ne} + ^{51}\text{V}$ system using recoil range measurement

Sabir Ali^{1,2,a}, Tauseef Ahmad¹, Kamal Kumar¹, I. A. Rizvi¹, Avinash Agarwal³, S. S. Ghugre⁴, A. K. Sinha⁴, and A. K. Chaubey⁵

¹Department of Physics, Aligarh Muslim University, Aligarh 202002, India

²Polytechnic Darbhanga, Maulana Azad National Urdu University, Hyderabad 500032, India

³Department of Physics, Bareilly College, Bareilly 243005, India

⁴UGC-DAE Consortium for Scientific Research, Kolkata 700098, India

⁵Department of Physics, Addis Ababa University, P.O.Box 1176, Addis Ababa, Ethiopia

Abstract. Recoil range distributions of evaporation residues, populated in $^{20}\text{Ne} + ^{51}\text{V}$ reaction at $E_{lab} \approx 145$ MeV, have been studied to determine the degree of momentum transferred through the complete and incomplete fusion reactions. Evaporation residues (ERs) populated through the complete and incomplete fusion reactions have been identified on the basis of their recoil range in the Al catcher medium. Measured recoil range of evaporation residues have been compared with the theoretical value calculated using the code SRIM. Range integrated cross section of observed ERs have been compared with the value predicted by statistical model code PACE4.

1 Introduction

In the last few years, study of nuclear reactions at energies near and above the Coulomb barrier have become an active topic of research [1–4]. Study of nuclear reaction around the barrier energy involves the investigation of complete and incomplete fusion processes and their dependence on various entrance channel parameters [5–8]. Complete fusion (CF) requires a total transfer of incident momentum from projectile to compound nucleus through the fusion of entire projectile's mass with the target. On the other hand, incomplete fusion (ICF) involves partial transfer of momentum from projectile to compound nucleus via the fusion of only a fraction of the incident projectile's mass with the target. Classically, either of these two processes will become feasible when the incident energy of projectile is higher than fusion barrier. Ever since the observation of the first ICF reaction by Britt and Quinton [9], numerous studies have been carried out to explore the mechanism involve in the ICF reactions. However, a real breakthrough was achieved by Inamura *et al.* [10] by performing the particle- γ coincidence measurements and claiming that ICF reactions were arising due to the break-up of incident projectile in peripheral collisions. It was suggested by Morgenstern *et al.* [11] and later on confirmed by several authors [5, 6, 12] that probability of ICF reaction increases with the increase in incident beam energy. This phenomenon of increase in ICF reaction probability with the incident beam energy was found to be a consequence of maximum angular momentum ℓ_{max} , associated with the

incoming projectile beam [13]. ℓ_{max} was found to be dependent on the incident beam energy through the relation [14],

$$\ell_{max} = R \sqrt{2\mu(E_{c.m} - V_B)/\hbar^2}. \quad (1)$$

where R is the maximum impact parameter at which the collision leads to a nuclear fusion reaction, and V_B is the fusion barrier. Liquid drop model based calculations have shown that the nuclear shape is distorted with increasing angular momentum until some critical value (ℓ_{crit}) is reached at which nuclear shape is no more stable [16, 17]. Thus, fusion is restricted by ℓ_{crit} above which no CF reaction is likely to occur. According to sumrule model, proposed by Wilczynski *et al.* [18], ICF reaction channels are localized in angular momentum space above ℓ_{crit} . At lower energies ℓ_{max} is close to ℓ_{crit} , thereby precluding any window for ICF reactions.

Following the CF or ICF reaction, an excited intermediate compound system is formed which decay to ground state via the emission of particles and/or γ -rays. The phenomenon of particle and/or γ -ray emission from the excited compound system is governed by the excitation energy of the compound system which in turn depends upon the degree of momentum transferred through the CF and/or ICF processes. Evaporation residues (ERs) populated through α -emitting channels can be populated through CF as well as ICF processes. There is no theoretical model proposed so far which could predict the exact fractional contribution arising from CF and/or ICF

^ae-mail: sabirjkh@gmail.com

Table 1. List of observed reaction channels populated in $^{20}\text{Ne} + ^{51}\text{V}$ reaction are given in first column along with the half-lives in the second column and other columns have spectroscopic properties taken from Ref.[19].

Reaction	Half-life	J^π	$E_\gamma(\text{keV})$	I^γ
$^{67}\text{Ge} (p3n)$	18.9 min	$1/2^-$	167.0 1472.5	84.4 4.9
$^{66}\text{Ge} (p4n)$	2.26 hrs	0^+	381.8 272.9	28.0 10.4
$^{65}\text{Ga} (\alpha 2n)$	15.2 min	$3/2^-$	115.0 153.0	54 8.9
$^{63}\text{Zn} (\alpha p3n)$	38.5 min	$3/2^-$	669.6 962.0	8.0 6.5
$^{62}\text{Zn} (\alpha p4n)$	9.18 hrs	0^+	596.5	26.0
$^{61}\text{Cu} (2\alpha 2n)$	3.33 hrs	$3/2^-$	282.9 656.0	12.2 10.7
$^{60}\text{Cu} (2\alpha 3n)$	23.7 min	2^+	1332.5 826.0	88.0 21.7
$^{61}\text{Co} (2\alpha 2p)$	1.65 hrs	$7/2^-$	908.6	3.6

processes in the formation of ERs populated through α -emitting channels. Measurements of recoil range distribution (RRD) of ERs populated through α -emitting channels was proved to be an important tool in determining the magnitude of contributions arising from each of the possible reaction dynamics. In the present work RRDs of eight ERs, namely $^{67}\text{Ge} (p3n)$, $^{66}\text{Ge} (p4n)$, $^{65}\text{Ga} (\alpha 2n)$, $^{63}\text{Zn} (\alpha p3n)$, $^{62}\text{Zn} (\alpha p4n)$, $^{61}\text{Cu} (2\alpha 2n)$, $^{61}\text{Co} (2\alpha 2p)$, and $^{60}\text{Cu} (2\alpha 3n)$ populated in the $^{20}\text{Ne} + ^{51}\text{V}$ reaction at $E_{lab} \approx 145$ MeV have been studied. A brief detail regarding the experimental setup used to perform the present work is given in section 2. Analysis and interpretation of the results are given in section 3 whereas the conclusion drawn from the observed results are given in the last section.

2 Experimental details

The present experiment was performed at Variable Energy Cyclotron Centre (VECC), Kolkata using $^{20}\text{Ne}^{6+}$ ion beam at energy $E_{lab} \approx 145$ MeV. The target used was ^{51}V foil (99.97% pure) of thickness $\approx 250 \mu\text{g}/\text{cm}^2$. The ^{51}V target was evaporated over an Al-backing of thickness $\approx 200 \mu\text{g}/\text{cm}^2$. The target-backing combination was mounted in a stack along with 20 thin Al-catcher foils, placed behind the target foil, to trap the recoiling nuclei. The thickness of each Al-catcher foil was determined prior to use by weighing as well as by the α -energy loss method, and it was found to range from 100 to 150 $\mu\text{g}/\text{cm}^2$. The projectile beam was collimated to a spot of diameter 8 mm and the beam current was found to be varying between 15-20 nA. The target was irradiated for a period of ≈ 11 hrs. The nuclear spectroscopic data used in the evaluation and measurement of the cross sections were taken from the Radioactive Isotopes Data Table of Brown and Firestone [19] and is given in Table 1 for ready reference. Details regarding the experimental setup were given in Ref. [20].

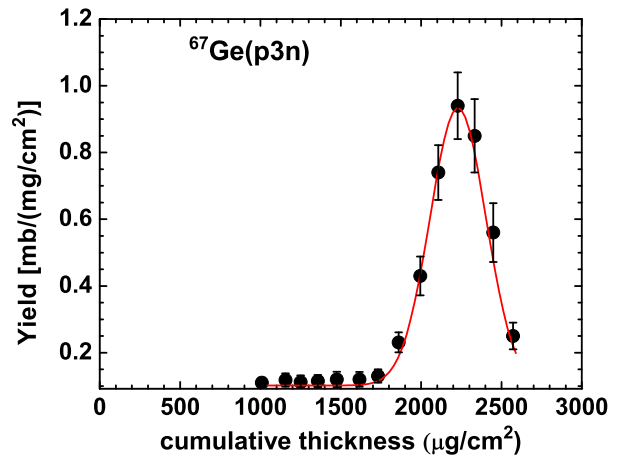


Figure 1. RRD of ER ^{67}Ge expected to be populated through the $p3n$ channel.

3 Results and analysis

The formation of ERs, populated through CF and/or ICF processes, consists of two stages. In the first stage, called ‘fusion stage’, an intermediate compound system is formed through the CF and/or ICF processes and the second stage, called ‘evaporation stage’, involves the de-excitation of the intermediate compound system through the particle and/or γ -ray emission. The intermediate compound system formed through the CF process will recoil in the Al catcher medium to a relatively larger recoil range as compared to the intermediate compound system formed through the ICF process. This discrepancy in recoil range of the intermediate compound systems formed through CF and ICF processes is arising due to the difference in degree of momentum transferred through the two processes.

3.1 RRDs of residues populated through pxn channel

CF of ^{20}Ne projectile with ^{51}V target leads to the formation of an excited intermediate compound system $^{71}\text{As}^*$. The excited intermediate compound system further decay via the emission of nucleons leading to the formation of $^{67,66}\text{Ge}$ isotope through the pxn ($x = 3, 4$) channels. As an example the systematics for the formation of ^{67}Ge through the CF process may be given as

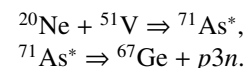


Fig. 1 shows the RRD of ER ^{67}Ge populated through $p3n$ channel. As can be seen from Fig. 1, RRD of ^{67}Ge residue consists of a single peak at $2229.6 \mu\text{g}/\text{cm}^2$ indicating the presence of complete momentum transfer from projectile to target through the CF process.

3.2 RRDs of residues populated through α emitting channels

ERs ^{65}Ga , ^{63}Zn , and ^{62}Zn populated through $\alpha 2n$, $\alpha p3n$, and $\alpha p4n$ channels, respectively can be populated through

Table 2. Experimental measured most probable range (R_{exp}) as well as theoretically calculated range (R_{theo}), using the code SRIM, in Al catcher foils in unit of $\mu\text{g}/\text{cm}^2$, for the experimentally observed reaction channels in $^{20}\text{Ne} + ^{51}\text{V}$ reaction at $E_{lab} \approx 145$ MeV.

Residues	CF		ICF $^\alpha$		ICF $^{2\alpha}$	
	R_{exp}	R_{theo}	R_{exp}	R_{theo}	R_{exp}	R_{theo}
^{67}Ge ($p3n$)	2229.6	2308	-	-	-	-
^{66}Ge ($p4n$)	2456.4	2308	-	-	-	-
^{65}Ga ($\alpha 2n$)	2200.6	2308	1457.8	1817	-	-
^{63}Zn ($\alpha p3n$)	2385.1	2308	1767.4	1817	-	-
^{62}Zn ($\alpha p4n$)	2396.1	2308	1665.9	1817	-	-
^{61}Cu ($2\alpha 2n$)	2354.9	2308	1817.1	1817	1304.2	1474
^{60}Cu ($2\alpha 3n$)	2304.0	2308	1853.1	1817	1424.4	1474
^{61}Co ($2\alpha 2p$)	2287.6	2308	1720.8	1817	1187.6	1474

CF as well ICF $^\alpha$ processes. The formation of α channel residues through the CF and ICF $^\alpha$ processes may be given by two different decay modes.

1. ICF $^\alpha$ Process: The ^{16}O nuclei, which forms through the α break-up of ^{20}Ne ($^{20}\text{Ne} \rightarrow ^{16}\text{O} + \alpha$), fuses with ^{51}V target leading to the formation of an incompletely fused composite system $^{67}\text{Ga}^*$ through the ICF $^\alpha$ process. $^{67}\text{Ga}^*$ further decay via the emission of nucleons leading to the formation of ERs ^{65}Ga , ^{63}Zn , and ^{62}Zn through the $2n$, $p3n$, and $p4n$ channels, respectively.

2. CF Process: CF of ^{20}Ne projectile with ^{51}V target leads to the formation of compound system $^{71}\text{As}^*$. ERs ^{65}Ga , ^{63}Zn , and ^{62}Zn have a finite probability of getting populated through the emission of $\alpha 2n$, $\alpha p3n$, and $\alpha p4n$, respectively from the excited compound system $^{71}\text{As}^*$.

3.3 RRDs of residues populated through 2α emitting channels

ERs ^{61}Cu , ^{60}Cu , and ^{61}Co were populated via $2\alpha 2n$, $2\alpha 3n$, and $2\alpha 2p$ channels, respectively. These 2α channel residues can be populated through CF, ICF $^\alpha$ as well as ICF $^{2\alpha}$ processes. The interplay between the contributions of CF, ICF $^\alpha$, and ICF $^{2\alpha}$ processes in the formation of ERs populated through 2α channel may be given as:

1. ICF $^{2\alpha}$ Process: ^{12}C , which forms through the 2α break-up of ^{20}Ne projectile ($^{20}\text{Ne} \rightarrow ^{12}\text{C} + ^8\text{Be}$), fuses with the ^{51}V target leading to the formation of an incompletely fused composite system $^{63}\text{Cu}^*$ through the ICF $^{2\alpha}$ process. The excited compound system $^{63}\text{Cu}^*$ further decay to ^{61}Cu , ^{60}Cu , and ^{61}Co residues through $2n$, $3n$, and $2p$ channels, respectively.

2. ICF $^\alpha$ Process: As mentioned before, due to break-up of ^{20}Ne projectile into ^{16}O and α -particle under the influence of target's field, $^{67}\text{Ga}^*$ was formed through the ICF $^\alpha$ Process. $^{67}\text{Ga}^*$ further decay via $\alpha 2n$, $\alpha 3n$, and $\alpha 2p$ channels leading to the formation of ERs ^{61}Cu , ^{60}Cu , and ^{61}Co , respectively.

3. CF Process: Excited compound system $^{71}\text{As}^*$, formed through the CF of ^{20}Ne projectile with ^{51}V target, may further decay via the emission of $2\alpha 2n$, $2\alpha 3n$, and

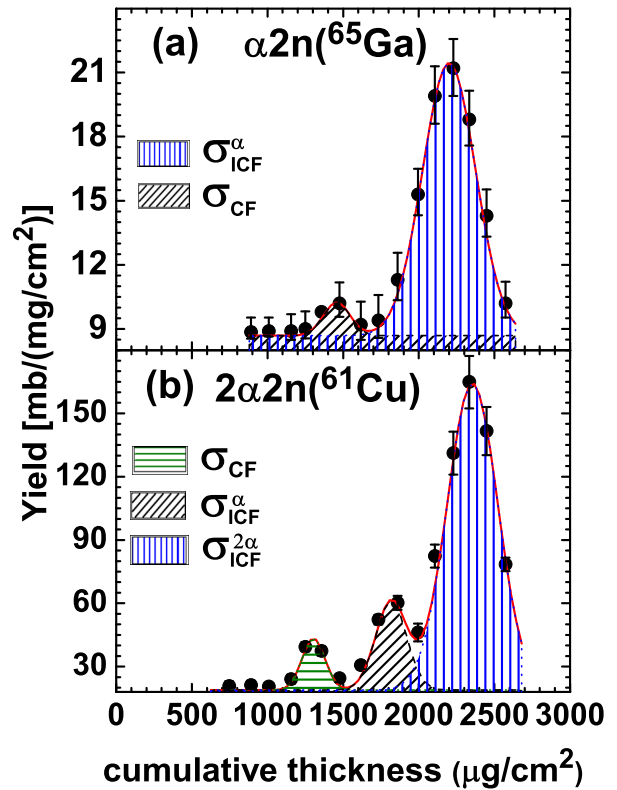


Figure 2. RRDs of ERs (a) ^{65}Ga , and (b) ^{61}Cu populated through $\alpha 2n$ and $2\alpha 2n$ channels respectively.

$2\alpha 2p$ to form the ERs ^{61}Cu , ^{60}Cu , and ^{61}Co , respectively. Fig. 2(a-b) shows the RRDs of ERs (a) ^{65}Ga , and (b) ^{61}Cu populated through $\alpha 2n$ and $2\alpha 2n$ channels, respectively. As can be seen from Fig. 2, the RRDs of ^{65}Ga consist of two peaks whereas RRDs of ^{61}Cu consists of three peaks, which is expected. The formation of ^{65}Ga through $\alpha 2n$ channel involves two different component of momentum transfer through the CF as well as ICF $^\alpha$ processes. On the other hand, the formation of ^{61}Cu through $2\alpha 2n$ channel involves three different components of momentum transfer through the CF, ICF $^\alpha$ and ICF $^{2\alpha}$ processes. The ex-

Table 3. Q value of the reaction products populated through CF, ICF $^\alpha$, and ICF $^{2\alpha}$ processes in the $^{20}\text{Ne} + ^{51}\text{V}$ reaction at $E_{lab} \approx 145$ MeV.

Residues	CF (MeV)	ICF $^\alpha$ (MeV)	ICF $^{2\alpha}$ (MeV)
$^{67}\text{Ge} (p3n)$	-28.09	-	-
$^{66}\text{Ge} (p4n)$	-37.21	-	-
$^{65}\text{Ga} (\alpha 2n)$	-15.15	-10.42	-
$^{63}\text{Zn} (\alpha p3n)$	-30.96	-26.23	-
$^{62}\text{Zn} (\alpha p4n)$	-40.07	-35.34	-
$^{61}\text{Cu} (2\alpha 2n)$	-18.34	-13.52	-6.36
$^{60}\text{Cu} (2\alpha 3n)$	-30.05	-25.23	-18.07
$^{61}\text{Co} (2\alpha 2p)$	-15.86	-11.04	-3.88

Table 4. Experimentally measured range integrated cross sections of ERs populated in $^{20}\text{Ne} + ^{51}\text{V}$ reaction at $E_{lab} \approx 145$ MeV along with the fusion cross section values calculated theoretically using the statistical model code PACE4.

Residues	σ_{RRD} (mb)	σ_{PACE4} (mb)
$^{67}\text{Ge} (p3n)$	0.56	0.92
$^{66}\text{Ge} (p4n)$	0.86	2.35
$^{65}\text{Ga} (\alpha 2n)$	22.30	10.70
$^{63}\text{Zn} (\alpha p3n)$	56.16	10.50
$^{62}\text{Zn} (\alpha p4n)$	45.37	19.10
$^{61}\text{Cu} (2\alpha 2n)$	114.92	109.00
$^{60}\text{Cu} (2\alpha 3n)$	30.53	5.10
$^{61}\text{Co} (2\alpha 2p)$	9.62	2.07

perimentally measured most probable range R_{exp} , along with the theoretically estimated value R_{theo} , estimated using the code SRIM [21] for all the identified ERs populated through the CF and/or ICF processes, are tabulated in Table 2. R_{theo} is estimated by assuming that ^{20}Ne projectile consist of five α -particles and the total incident momentum is equally distributed among its five α constituents.

Table 3 gives the Q value of the observed ERs populated through the CF, ICF $^\alpha$ and ICF $^{2\alpha}$ processes in the $^{20}\text{Ne} + ^{51}\text{V}$ reaction. Table 4 gives the range integrated experimentally measured reaction cross section of ERs populated in $^{20}\text{Ne} + ^{51}\text{V}$ reaction at $E_{lab} \approx 145$ MeV. Last column of Table 4 gives the theoretically estimated values of reaction cross section, calculated using the statistical model code PACE4 [22]. It can be inferred from Table 4 that experimental reaction cross section of residues populated through the pxn channels are in good agreement with the PACE4 predictions, whereas the reaction cross section of α channel residues shows an enhancement over the PACE4 values. Such type of result is expected since the statistical

model code PACE4 does not take ICF reactions into account.

4 Conclusion

The RRDs of eight radionuclides, namely $^{67}\text{Ge}(p3n)$, $^{66}\text{Ge}(p4n)$, $^{65}\text{Ga}(\alpha 2n)$, $^{63}\text{Zn}(\alpha p3n)$, $^{62}\text{Zn}(\alpha p4n)$, $^{61}\text{Cu}(2\alpha 2n)$, $^{60}\text{Cu}(2\alpha 3n)$, and $^{61}\text{Co}(2\alpha 2p)$, populated in $^{20}\text{Ne} + ^{51}\text{V}$ reaction at $E_{lab} \approx 145$ MeV have been studied. The analysis of measured RRDs of ERs populated through α -emitting channels reveal a significant contribution of partial momentum transfer from incident projectile to target. Different partial momentum transfer components were attributed to the fusion of ^{16}O and ^{12}C , formed through the break-up of ^{20}Ne projectile, with the ^{51}V target nucleus.

References

- [1] P. R. S. Gomes *et al.*, Phys. Rev. C **73**, 064606 (2006)
- [2] M. Dasgupta *et al.*, Phys. Rev. C **70**, 024606 (2004)
- [3] V. Tripathi *et al.*, Phys. Rev. Lett. **88**, 172701 (2002)
- [4] M. Dasgupta *et al.*, Phys. Rev. C **82**, 1395 (1999)
- [5] Kamal Kumar *et al.*, Phys. Rev. C **88**, 064613 (2013)
- [6] Kamal Kumar *et al.*, Phys. Rev. C **87**, 044608 (2013)
- [7] Avinash Agarwal *et al.*, Eur. Phys. J. Web of Conference **38**, 17001 (2012)
- [8] Tauseef Ahmad *et al.*, Int. J. Mod. Phys. E **20**, 645 (2011)
- [9] H. C. Britt, A. R. Quinton, Phys. Rev. **124**, 877 (1961)
- [10] T. Inamura *et al.*, Phys. Lett. B **68**, 51 (1977)
- [11] H. Morgenstern *et al.*, Z. Phys. A **313**, 39 (1983)
- [12] Abhishek Yadav *et al.*, Phys. Rev. C **86**, 014603 (2012)
- [13] S. Mukherjee *et al.*, Eur. Phys. J. A. **12**, 199 (2001)
- [14] J. Wilczynski, Nucl. Phys. A **216**, 465 (1973)
- [15] J. Wilczynski *et al.*, Phys. Rev. Lett. **45**, 606 (1980)
- [16] R. Beringer, W. J. Knox, Phys. Rev. **121**, 1195 (1961)
- [17] B. N. Kalinkin, I. Z. Petkov, Acta. Phys. Polon **25**, 265 (1964)
- [18] J. Wilczynski *et al.*, Phys. Rev. Lett. **45**, 606 (1980)
- [19] E. Browne, R. B. Firestone, Table of Radioactive Isotopes(Wiley, New York, 1986)
- [20] F. K. Amanuel *et al.*, Eur. Phys. J. A **47**, 156 (2011)
- [21] J. F. Ziegler, SRIM-2006, The Stopping Power and Range of Ions in Matter [<http://www.srim.org/SRIM/SRIMLEGL.htm>]
- [22] A. Gavron, Phys. Rev. C **21**, 230 (1980)